



## Effect of Cement Plaster and Insulation Materials on the Thermal Performance of Masonry Wall

Noor Nabilah Sarbini<sup>1,\*</sup>, Liew Chia Ming<sup>1</sup>, Izni Syahrizal Ibrahim<sup>1</sup>, Nor Fazlin Zamri<sup>1</sup>, Reni Suryanita<sup>2</sup>

<sup>1</sup> Faculty of Civil Engineering, Universiti Teknologi Malaysia, 81310 Skudai, Johor, Malaysia

<sup>2</sup> Civil Engineering Department, Faculty of Engineering, Universitas Riau, Pekanbaru Riau 28293 Indonesia

### ARTICLE INFO

#### Article history:

Received 22 February 2024

Received in revised form 15 October 2024

Accepted 15 December 2024

Available online 31 December 2024

#### Keywords:

Insulation material; clay brick; thermal performance; masonry wall

### ABSTRACT

The thermal performance of masonry walls plays a critical role in maintaining indoor comfort and minimizing energy consumption. However, in many developing countries, construction practices often overlook the importance of thermal insulation and mass, leading to inefficient energy use in buildings. This study investigates the effect of cement plaster thickness and insulation materials on the thermal properties of masonry walls constructed from clay bricks. The primary objective is to assess how varying plaster thickness and the inclusion of insulation materials impact thermal conductivity and heat transfer. Two methods were employed for data collection: the use of thermocouples to measure spot temperature differences and a thermal imaging camera to create surface temperature maps. The findings reveal that thicker cement plaster and insulation materials, particularly polystyrene boards, enhance the wall's thermal resistance, reducing heat transfer. Specifically, a 20mm polystyrene board reduced heat transmission by up to 51.7%. These results underscore the importance of integrating effective insulation materials in building design to promote energy efficiency and improve thermal comfort. Further research into innovative insulation solutions is recommended to optimize performance and cost-effectiveness.

## 1. Introduction

Clay bricks are known for providing superior insulation compared to other building materials, making bricks the ideal and most energy-efficient choice for construction [1]. However, in many developing countries, there is a limited consideration of thermal insulation and thermal mass in construction practices [2,3]. It is essential to extend the focus on energy conservation and efficiency to the construction industry [4]. Thermal insulation of masonry walls is crucial, as it helps maintain a consistent and comfortable indoor temperature [5]. A well-insulated masonry wall can minimize unwanted heat loss or gain, thus reducing the energy requirements of heating and cooling systems [6,7]. Therefore, achieving thermal comfort and energy efficiency is a paramount consideration in

\* Corresponding author.

E-mail address: [noornabilah@utm.my](mailto:noornabilah@utm.my)

<https://doi.org/10.37934/ard.123.1.248260>

masonry wall design. Designers must actively promote the concept of low-energy building construction by adopting energy-efficient construction materials [8], particularly for walls.

Srimuang *et al.*, [9] conducted a study on innovative hybrid sandwich insulated panels to enhance the thermal comfort of four case study houses in Thailand. Their research revealed that these innovative panels significantly improved thermal performance. In recent years, there has been increased interest in building insulation to address energy consumption concerns. Brick, as a construction material, remains a prominent choice for wall components [10-12]. While previous research has examined the thermal performance of various brick types and wall configurations, there is still a need for more information regarding masonry walls and their response to external factors [10-12]. Although cement plaster provides some level of thermal insulation, it is not as effective as clay bricks, and its thermal properties are influenced by thickness. Furthermore, questions arise about the extent of insulation achievable with plaster, even when using insulation materials.

Thermal conductivity refers to a material's inherent ability to conduct or transport heat [13]. In a wall, thermal conductivity occurs through molecular agitation and contact, rather than bulk movement of the solid material. Heat travels along a temperature gradient, from areas with high temperature and molecular energy to those with lower temperature and lower molecular energy [10]. This heat transfer continues until thermal equilibrium is reached. The rate of heat transmission depends on the temperature gradient and the material's specific thermal properties [11]. Additionally, thermal conductivity is influenced by factors such as operational temperature, moisture content, and macroscopic density [12].

Thermal mass, also known as heat capacity, is the capacity of a material to absorb, store, and release heat. It plays a crucial role in space cooling, as it helps maintain stable temperatures over longer periods, acts as a natural barrier between indoor and outdoor temperatures, and enhances thermal comfort [14]. When considering thermal mass, it is important to factor in thermal lag, which is the rate at which a material absorbs and emits heat. Materials with significant thermal lag times, such as brick and concrete, have slow heat absorption and release, whereas those with short lag times, like steel, quickly absorb and release heat [15].

Thermal insulation measures the resistance of insulation batts to heat transfer. It defines the material's ability to resist the passage of heat from one side to another [16]. The rate of heat transfer through a masonry wall depends on the temperature difference between the sides, thickness, and contact area. It is directly proportional to temperature and contact area, with thicker walls providing greater resistance to heat flow [17-19].

The thermal properties of bricks are crucial for a building's thermal performance [20]. Masonry buildings often offer higher thermal performance compared to light-frame buildings with equivalent insulation ratings due to their significant thermal energy storage capacity. However, to achieve substantial overall thermal resistance, additional insulation methods like cement plaster and insulation fillings are still necessary in masonry wall assemblies. Different brick shapes and types are introduced to the market to minimize the reduction in thermal resistance, enhance thermal design, and reduce building energy consumption. However, there is a gap in the understanding of how varying cement plaster thickness and specific insulation materials, impact heat transfer and thermal resistance in masonry walls. This study is significant as it fills the knowledge gap on how cement plaster thickness and insulation materials affect the thermal performance of masonry walls, providing insights for improving energy efficiency and guiding the construction industry towards better, cost-effective insulation strategies. Thus, this research aims to investigate the thermal performance of masonry walls while considering cement plaster thickness and the presence of insulation material, employing two different testing methods. It also compares the results obtained through thermocouple measurements and thermal camera tests to analyze differences. The study's scope

includes laboratory tests and analysis to determine the properties of masonry walls, including temperature differences, heat transfer amounts, thermal conductivity, and thermal resistance.

## 2. Methodology

A series of laboratory tests were conducted on a masonry wall with varying plaster thickness and the presence of insulation material. This research was preceded by a study on wall sample preparation and the test procedure. Two main apparatus, a thermal camera, and thermocouples were used to determine the thermal performance of the tested masonry walls. The results were determined by comparing thermal properties between different sets of tested wall samples. The first parameter in the thermal test of masonry walls is the plaster thickness, ranging from 20 mm of one-sided plaster to 20 mm of two-sided plaster, while the presence of the insulation material (polystyrene board) serves as the second parameter.

### 2.1 Physical and Mechanical Properties Tests of Clay Bricks

Five clay bricks were tested for compressive strength to determine their load-carrying capacity when subjected to a compressive load at a uniform rate of  $14 \text{ N/mm}^2$ . The maximum load at failure was recorded and divided by the cross-sectional area of the bricks to calculate their compressive strength. The second mechanical property examined was the water absorption of clay bricks. Five brick samples underwent water absorption tests. The dry weight and the weight of clay bricks after 24 hours of immersion were recorded, and water absorption was calculated by dividing the weight difference by the dry weight.

For the design of the wall specimens, it was proposed that the exposed area should be at least  $0.25 \text{ m}^2$  with a surface dimension of  $0.5 \text{ m} \times 0.5 \text{ m}$  and a thickness of 100 mm without the cement plaster. The proposed wall bond type is the stretcher bond. In the thermal test of masonry walls, the first parameter is the thickness of cement plaster. The thermal test on the masonry wall is conducted with the influence of cement plaster: without plaster (specimen A), with 20mm of one-sided plaster (specimen B), and with 20 mm of two-sided plaster (specimen C). The composition of the cement plaster is 1:4 (1 part cement and 4 parts of sand that passed through a sieve with 2.36 mm openings). A 20 mm thick polystyrene board is then attached to the wall (specimen D) as the second parameter in this thermal test. Figure 1 illustrates the dimensions of the wall specimens.

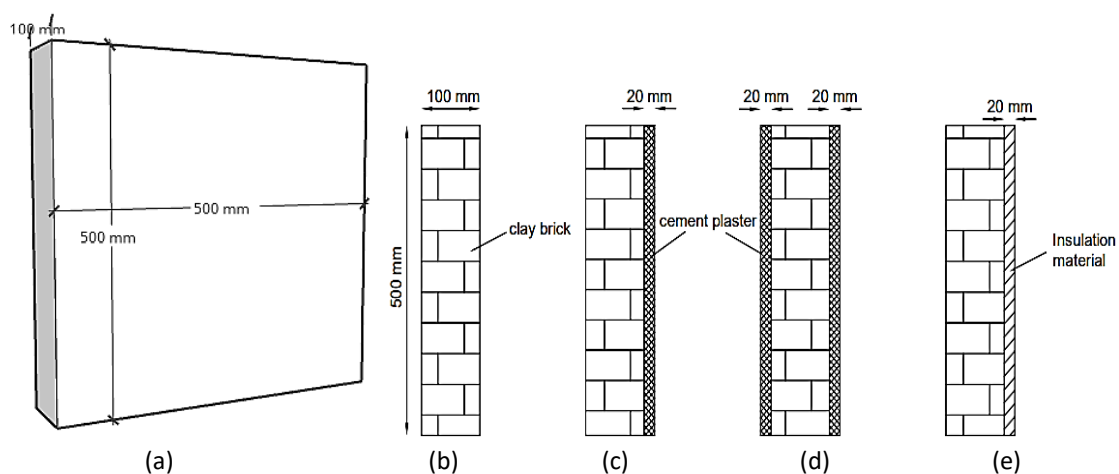


**Fig. 1.** Wall specimens (a) Wall dimension, (b) Specimen A, (c) Specimen B, (d) Specimen C and (e) Specimen D

## 2.2 Thermal Test of Masonry walls

The four wall sides depicted in Figure 2 were assembled to create a square structure with an opening in the center to accommodate the thermal source. A 100-watt incandescent bulb is positioned in the middle of the setup to provide consistent thermal energy to the surrounding walls as shown in Figure 3. A cover, consisting of polystyrene board and plywood, was placed on top to minimize heat loss during the thermal test. This setup offers several advantages, including the ability to conduct thermal tests on all four walls simultaneously in an enclosed environment, ensuring that each of the four walls receives the same thermal energy when the thermal source is positioned in the center. For the thermal test, two approaches were employed to measure the temperature difference between each wall specimen, denoted as methods 1 and 2, as outlined below to ensure the validity of the results. The thermal test was repeated three times to obtain an average temperature difference value. The duration of each round of the thermal test was 90 minutes.

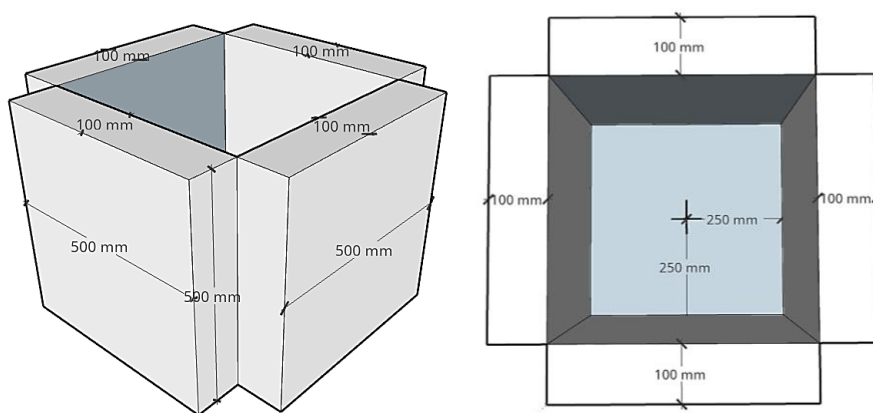


**Fig. 2.** Schematic diagram for the test set-up

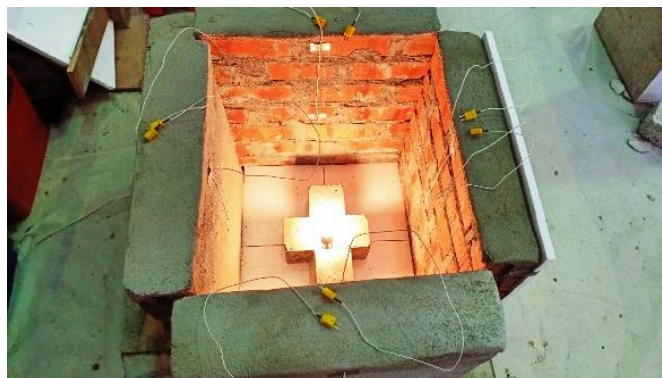


**Fig. 3.** Thermal test of masonry walls

## 2.3 Thermal Test

### 2.3.1 Method 1: Thermocouples and thermometer

A pair of Type-K thermocouples was first attached to both surfaces of each wall specimen before lighting up the thermal source. Next, a thermometer model UT320D was used to connect to each pair of thermocouples after 90 minutes of the thermal test to measure the temperature at each surface. The temperature measured at the wall surface that is exposed to heat was labeled as  $T_{spot,1}$  and  $T_{spot,2}$  for the surface that is away from the thermal source. The temperature difference measured by this

method is the spot temperature difference,  $\Delta T_{spot}$ , as the thermocouple is only capable of measuring the temperature at one specific point, as shown in Figure 4.

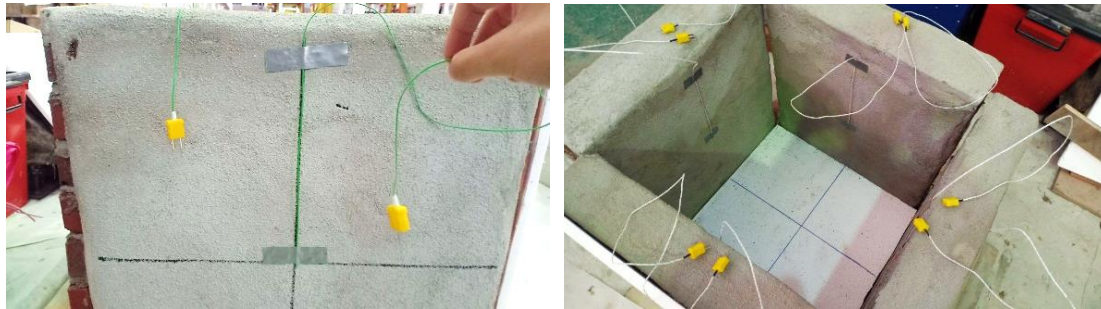


**Fig. 4.** Test setup for method 1

### 2.3.2 Method 2: Thermal imaging camera and flir studio software analysis

A compacting thermal imaging camera was introduced as method 2 to ensure the validity of the study. A thermal imaging camera Flir Cx-Series was then used to take the thermal image of all the wall specimens on both surfaces before and after the thermal test. The thermal images were then analyzed using a thermal reporting software named Flir Thermal Studio to derive the surface temperature of each wall specimen. The surface temperature of the wall that is exposed to the thermal source was labeled as  $T_{surface,1}$  and  $T_{surface,2}$  for the surface temperature of the wall that is away from the thermal source. The surface temperature differences,  $\Delta T_{surface}$ , were then determined. In the thermal test, the spot temperature difference,  $\Delta T_{spot}$  and the surface temperature difference,  $\Delta T_{surface}$  between masonry walls for every configuration were measured by using thermocouples and thermal mapping analysis. The amount of heat transferred for each case can be determined using the following formula as shown in Eq. (1) to (3).

$$Q = keff \cdot A \cdot \frac{\Delta T}{d} \quad (1)$$

Where  $Q$  = amount of heat transfer (W),  $keff$  = effective thermal conductivity ( $W \cdot m^{-1} \cdot K^{-1}$ ),  $d$  = wall thickness (m),  $A$  = wall surface area ( $m^2$ ), and  $\Delta T$  = temperature differences =  $\Delta T_{spot}$  or  $\Delta T_{surface}$ . The effective conductivity of multi-layered composite materials (specimens B, C and D) is the weighted mean of each component layer's conductivity, where the weight is the cross-sectional area of each layer. Thus, the effective conductivity:

$$keff = \frac{\sum ki \cdot Ai}{\sum Ai} \quad (2)$$

Where  $keff$  = effective thermal conductivity ( $W \cdot m^{-1} \cdot K^{-1}$ ),  $ki$  = thermal conductivity of each layer ( $W \cdot m^{-1} \cdot K^{-1}$ ), and  $Ai$  = surface area of each layers ( $m^2$ ). The thermal resistance of each case of wall was then calculated by using the formula where,  $R$  = thermal resistance ( $m^2 \cdot K \cdot W^{-1}$ ); and  $d$  = wall thickness (m).

$$R = d/keff \quad (3)$$

### 3. Results

#### 3.1 Mechanical Properties of Clay Brick

Fired clay bricks demonstrate a high compressive strength, typically ranging from 20 to 40 N/mm<sup>2</sup>. The average compressive strength of the clay bricks utilized in this research is 34.4 N/mm<sup>2</sup>, which is generally suitable for domestic construction. Furthermore, the clay bricks used are classified as first-class bricks, with a water absorption rate of 11.6%. It is important to note that for first-class bricks, the water absorption should not exceed 20%, while second-class bricks can have up to 22% water absorption, and third-class bricks may have up to 25% water absorption. The results are summarized in Table 1.

**Table 1**  
 Summary of the mechanical properties of tested clay brick

| Properties           | Description                          | Acceptance range                               |
|----------------------|--------------------------------------|--|
| Brick type           | Common fired clay brick              | -  |
| Length               | 210 mm                               | 190 mm-220 mm                                  |
| Width                | 100 mm                               | 90 mm-110 mm                                   |
| Thickness            | 70 mm                                | 70 mm-90 mm                                    |
| Volume               | 1.47×10 <sup>-3</sup> m <sup>3</sup> | Depend on size                                 |
| Dry weight           | 2.80 kg                              | < 3.5 kg                                       |
| Density              | 1905 kg/m <sup>3</sup>               | 1600 kg/m <sup>3</sup> -1900 kg/m <sup>3</sup> |
| Compressive strength | 34.4 N/mm <sup>2</sup>               | < 40 N/mm <sup>2</sup> (first class)           |
| Water absorption     | 11.6 %                               | < 20% (first class)                            |

#### 3.2 Spot Temperature Difference, $\Delta T_{spot}$ (Method 1)

Specimen A consistently exhibits the smallest spot temperature difference, with specimen B following closely in every round of the thermal test. Notable variations are observed in specimens C and D. Specimen C records the highest spot temperature difference in the first round, while specimen D attains the highest in the subsequent two rounds of the test. This finding was further examined, and a comparative analysis with method 2 was conducted to assess whether both methods yield similar observations. The highest amount of heat transfer is observed in Specimen A, followed by Specimens B, C, and D, as detailed in Tables 2 and 3.

**Table 2**  
 Spot temperature difference,  $\Delta T_{spot}$

| Wall specimen | $\Delta T_{spot}$ (°C) |         |         |         |
|---------------|------------------------|---------|---------|---------|
|               | Round 1                | Round 2 | Round 3 | Average |
| A             | 1.60                   | 2.50    | 1.90    | 2.00    |
| B             | 1.90                   | 3.40    | 2.50    | 2.60    |
| C             | 4.10                   | 4.60    | 4.20    | 4.30    |
| D             | 3.00                   | 5.10    | 4.30    | 4.13    |

**Table 3**  
 Amount of heat transferred, Q

| Wall specimen | Q (W)   |         |         |         |
|---------------|---------|---------|---------|---------|
|               | Round 1 | Round 2 | Round 3 | Average |
| A             | 831.12  | 833.84  | 832.03  | 832.33  |
| B             | 589.35  | 592.57  | 590.64  | 590.85  |
| C             | 479.25  | 480.11  | 479.42  | 479.59  |
| D             | 400.27  | 403.32  | 402.16  | 401.92  |

### 3.3 Surface Temperature Difference, $\Delta T_{surface}$ (Method 2)

The surface temperature differences, and the amount of heat transferred obtained through the thermal compacting camera and software analysis are shown in Figure 5. The results are in Tables 4 and 5.

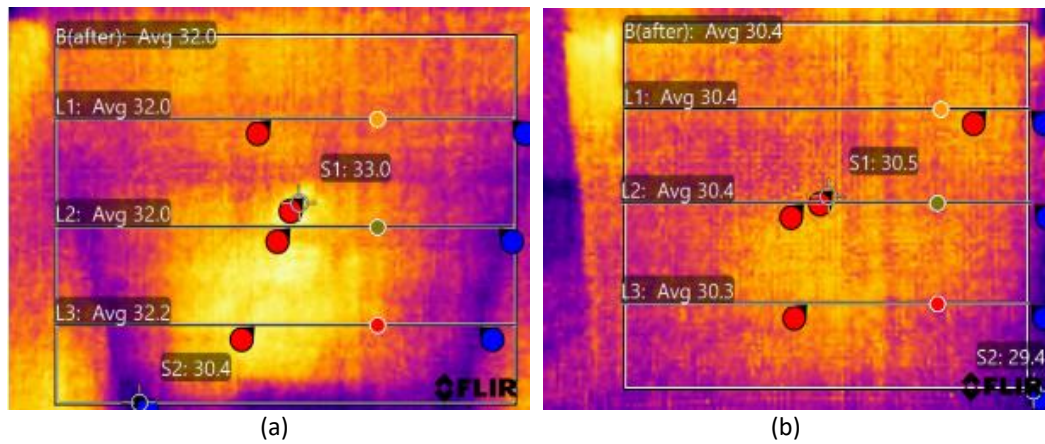


**Fig. 5.** Surface temperature of specimen A of both surfaces using thermal mapping analysis (a) Wall surface that exposed to the thermal source an (b) Opposite wall surface

**Table 4**

Surface temperature difference,  $\Delta T_{surface}$

| Wall specimen | $\Delta T_{surface}$ (°C) |         |         |         |
|---------------|---------------------------|---------|---------|---------|
|               | Round 1                   | Round 2 | Round 3 | Average |
| A             | 1.60                      | 2.00    | 1.90    | 1.83    |
| B             | 2.30                      | 3.10    | 2.40    | 2.60    |
| C             | 4.50                      | 4.30    | 3.10    | 3.97    |
| D             | 3.60                      | 5.00    | 4.00    | 4.20    |

**Table 5**

Amount of heat transferred, Q

| Wall specimen | Q (W)   |         |         |         |
|---------------|---------|---------|---------|---------|
|               | Round 1 | Round 2 | Round 3 | Average |
| A             | 831.12  | 832.33  | 832.03  | 831.83  |
| B             | 590.21  | 591.92  | 590.42  | 590.85  |
| C             | 479.94  | 479.59  | 477.52  | 479.13  |
| D             | 401.14  | 403.17  | 401.72  | 402.01  |

### 3.4 Comparison Between Method 1 and Method 2

In Method 1, Specimen C with 20 mm two-sided cement plaster achieved the highest average spot temperature difference,  $\Delta T_{spot}$ , up to 4.3°C, followed by Specimen D with 4.1°C, Specimen B with 2.6°C, and lastly Specimen A with 2.0°C. However, in Method 2, Specimen D with a 20 mm polystyrene board is observed to have the highest average surface temperature difference,  $\Delta T_{surface}$ , up to 4.2°C. In both methods, Specimen A achieved the lowest temperature difference, which is 2.0°C for spot temperature and 1.8°C for surface temperature difference, respectively. Besides, Specimen B with the 20 mm one-sided cement plaster had the same value of temperature difference, 2.6°C in both methods. Based on the results, it can be seen that a 20 mm polystyrene board has a better tendency to restrain the heat transfer in all directions compared to the 20 mm one-sided and two-sided cement

plaster. This is indicated by the highest average surface temperature observed. However, a 20 mm two-sided cement plaster is observed to have a better tendency than the 20 mm polystyrene board to restrain the heat transfer in a longitudinal direction at a particular spot because it has the highest average spot temperature difference. The results are summarized in Table 6.

**Table 6**

Average value of the temperature differences,  $\Delta T$  and the amount of heat transfer,  $Q$

| Wall specimen | Method 1  |         | Method 2   |         |
|---------------|---|---------|--|---------|
|               | $\Delta T_{\text{spot}}$ ( $^{\circ}\text{C}$ ) | $Q$ (W) | $\Delta T_{\text{surface}}$ ( $^{\circ}\text{C}$ ) | $Q$ (W) |
| A             | 2.00  | 832.33  | 1.83   | 831.83  |
| B             | 2.60  | 590.85  | 2.60   | 590.85  |
| C             | 4.30  | 479.59  | 3.97   | 479.13  |
| D             | 4.13  | 401.92  | 4.20   | 402.01  |

Figures 6(a) and 6(b) shows the amount of heat transferred across the wall specimen of methods 1 and 2, respectively. Both methods have the same trend that specimen A has the highest amount of heat transferred followed by specimens B, C, and D. These results demonstrate that the cement plasters and the polystyrene have a significant impact on the thermal performance of masonry wall. The 20 mm polystyrene board was proven to have the greatest insulation properties since the least heat is transferred after the 90-minutes exposure to the thermal source followed by 20 mm two-sided and 20 mm one-sided cement plaster.

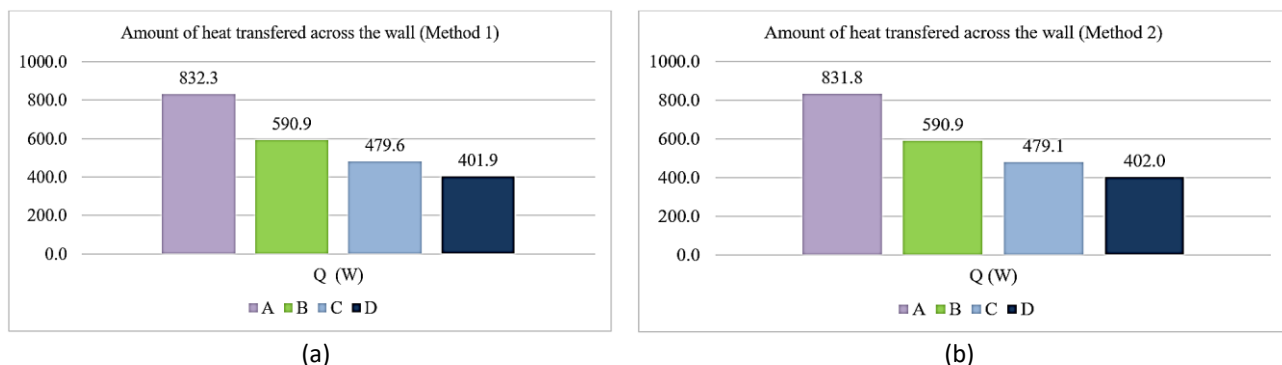


**Fig. 6.** Amount of heat transferred across the wall (a) Method 1 (b) Method 2

### 3.5 Effect of Cement Plaster Thickness and Insulation Material

Table 7 provides an overview of the thermal properties of wall specimens A, B, C, and D, considering the average values from both methods 1 and 2. Specimen B has a 20 mm cement plaster applied to the surface exposed to the thermal source, and this composite material consists of a layer of cement plaster and clay brick. Several factors contribute to the reduction in heat transfer rate in Specimen B compared to Specimen A. (1) Thickness: specimen B has a 20 mm greater thickness compared to Specimen A, which inherently reduces the rate of heat transmission. (2) Cement plaster: the presence of cement plaster is a crucial factor in limiting heat transfer. Specimen B demonstrates a 29% reduction in heat transfer compared to a wall without cement plaster as shown in Table 8. The cement plaster in this case consists of Ordinary Portland Cement and fine sand. Specimen C takes this a step further by increasing both wall thickness and the number of voids, further restricting the flow of heat across the wall. This results in a larger reduction in heat transfer, up to 42.4%. Specimen D, featuring a 20 mm polystyrene board, is the most effective approach in terms of insulation



properties. It boasts the highest thermal resistance value of 0.21 m<sup>2</sup>K/W and can reduce heat energy transmission by 51.7% compared to Specimen A.

Furthermore, Specimen C exhibits the lowest effective thermal conductivity at only 0.58 W/mK, indicating the lowest rate of heat transfer across the specimen. These findings highlight the significant impact of insulation materials and thickness on thermal performance.

**Table 7**

Average value of the thermal properties of masonry walls

| Wall specimen | Temperature differences, $\Delta T$ (°C) | Heat transferred, Q (W) | Effective thermal conductivity, $k_{eff}$ (W/mK) | Thermal resistance R (m <sup>2</sup> K/W) |
|---------------|--|-------------------------|--|---|
| A             | 1.92                                     | 832.08                  | 1.00   | 0.10                                      |
| B             | 2.60                                     | 590.85                  | 0.85   | 0.14                                      |
| C             | 4.14                                     | 479.36                  | 0.80   | 0.18                                      |
| D             | 4.17                                     | 401.97                  | 0.58   | 0.21                                      |

**Table 8**

Percentage reduction of the amount of heat as compared to specimen A (control)

| Parameter           | Wall specimen                | Percentage reduction of heat transferred (%) |
|---------------------|------------------------------|--|
| Cement plaster      | B - 20mm one sided plastered | 29.0   |
|                     | C - 20mm two sided plastered | 42.4   |
| Insulation material | D - 20mm polystyrene board   | 51.7   |

Figure 7 illustrates the relationship between the amount of heat transferred and the measured temperature differences for each specimen. It is important to note that the temperature differences measured act as the responding variable in this context. In the graph, it becomes evident that specimens with a larger amount and a higher rate of heat transfer tend to reach thermal equilibrium more quickly. This equilibrium results in a smaller temperature difference between the two wall surfaces once both surfaces have reached a similar temperature. For instance, Specimen A, which lacks both cement plaster and insulation material, exhibits the highest thermal conductivity, leading to the largest amount of heat transferred. Consequently, it requires a shorter time to reach thermal equilibrium between both surfaces, resulting in the smallest temperature difference. In contrast, Specimen D, which has a 20 mm polystyrene board, demonstrates a smaller amount of heat transferred within the same test duration compared to Specimen A. This reduced heat transfer contributes to a slower achievement of thermal equilibrium and a larger temperature difference. This relationship between heat transfer and temperature differences is an essential aspect of understanding the thermal performance of the specimens.

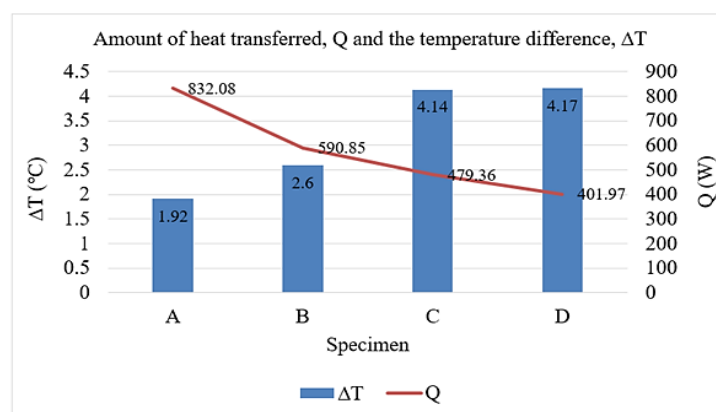


**Fig. 7.** Relationship between the amount of heat transferred and the temperature differences measured

Figure 8(a) illustrates the relationship between the effective thermal conductivity and the amount of heat transferred across the masonry wall, considering the thickness of cement plaster. This relationship demonstrates a clear trend: the higher the value of effective conductivity, the greater the amount of heat transferred through the walls. When cement plaster is applied to the wall (specimen B), it results in a decrease in effective thermal conductivity, which in turn limits the heat transfer. As the thickness of the cement plaster is increased (specimen C), the thermal conductivity further decreases, effectively restricting more heat transfer across the two wall surfaces. Thus, it is evident that increasing the thickness of the applied cement plaster leads to a lower effective conductivity. Figure 8(b) shows how the presence of insulation material, such as the polystyrene board used in specimen D, can significantly reduce the effective conductivity and heat transfer. The polystyrene board, characterized by a high void-to-solid ratio, effectively lowers the thermal conductivity of the wall as a composite material. This is because voids or gases within the insulation material have poor thermal conduction properties compared to solid materials. As a result, the insulation material acts as a barrier, decreasing the rate of thermal conduction and limiting heat transmission.

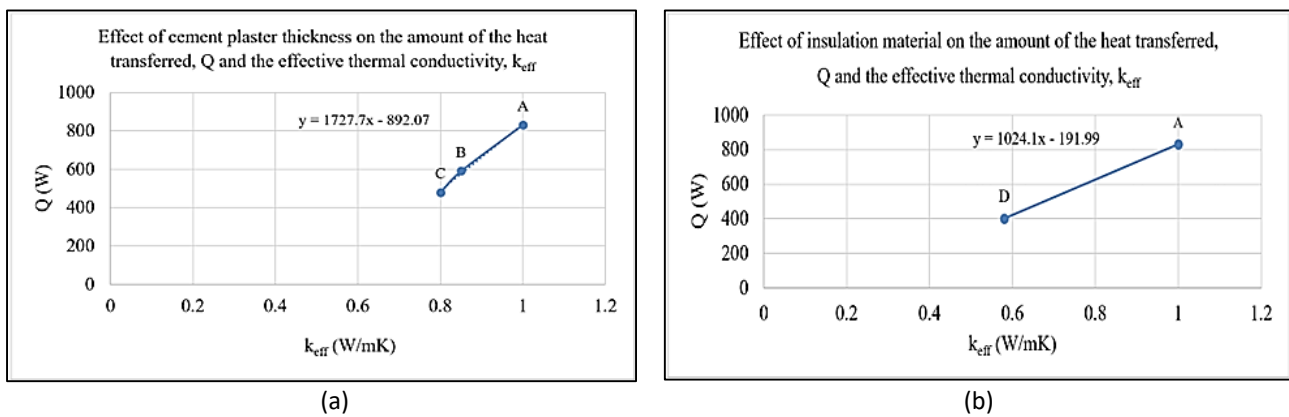
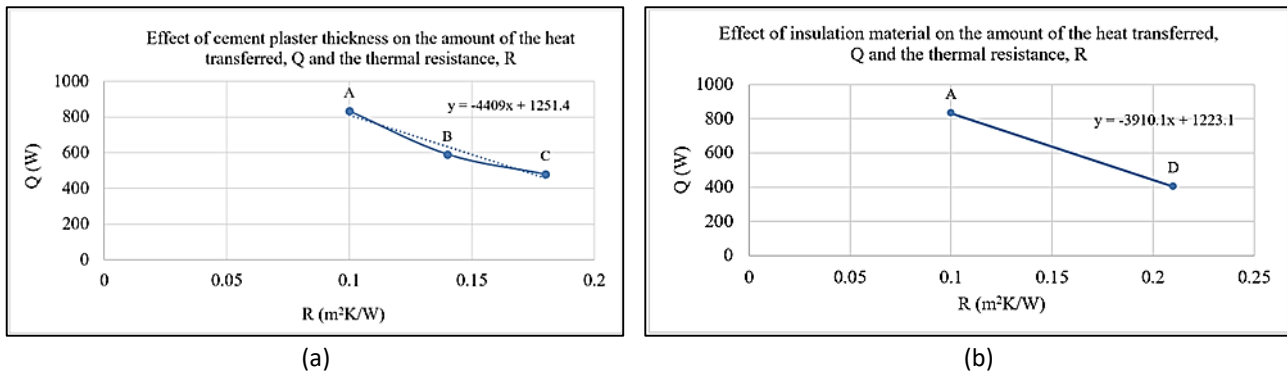


Fig. 8. (a) Effect of cement plaster thickness and (b) Effect of insulation material on  $k_{eff}$  and  $Q$

The thickness of the cement plaster applied results in a higher thermal resistance value, leading to a reduction in the amount of heat transferred. The thermal resistance is defined as the ratio of the temperature difference between two wall surfaces to the rate of heat flow per unit area. With a constant area of wall specimens, a higher temperature difference indicates a larger thermal resistance and a smaller rate of heat flow. Specimen C, which has the greatest thickness of cement plaster applied, demonstrates a smaller rate of heat flow per unit area. This implies that the thermal resistance of the masonry wall is directly proportional to the thickness of the cement plaster applied. In other words, the thicker the cement plaster applied, the more effective it is at preventing heat from being transmitted to the other surface. Figure 9(a) illustrates that attaching an insulation material to the wall specimen increases its insulation properties, resulting in a reduction in the heat transferred across the masonry wall. This is consistent with Figure 9(b), where a higher thermal resistance corresponds to a smaller amount of heat transferred. The particles within the polystyrene board do not easily move when exposed to thermal energy, thanks to the strong bond that rigidly holds the particles in place. Consequently, the amount of heat transferred is minimized, effectively increasing the thermal resistance of the wall.



**Fig. 9.** (a) Effect of cement plaster thickness (b) Effect of insulation material on R and Q

Figure 10 illustrates the relationship between effective thermal conductivity and thermal resistance. Thermal conductivity measures how much heat passes through the wall specimens, while thermal resistance measures the ability of the wall to resist heat from passing through. The trend line pattern in Figure 10 shows that thermal resistance is inversely proportional to thermal conductivity. This relationship is consistent with the formulation that thermal resistance is calculated by dividing the thickness of the wall specimens by their thermal conductivity. In this research, both cement plaster and polystyrene board are shown to reduce the thermal conductivity and increase the thermal resistance of the masonry wall, assuming a constant surface area exposed to the thermal source. Therefore, it can be concluded that cement plaster and insulation board are effective and practical for thermal insulation. They significantly increase the resistance to heat flow, helping to maintain the desired temperature in a building and improve overall comfort.

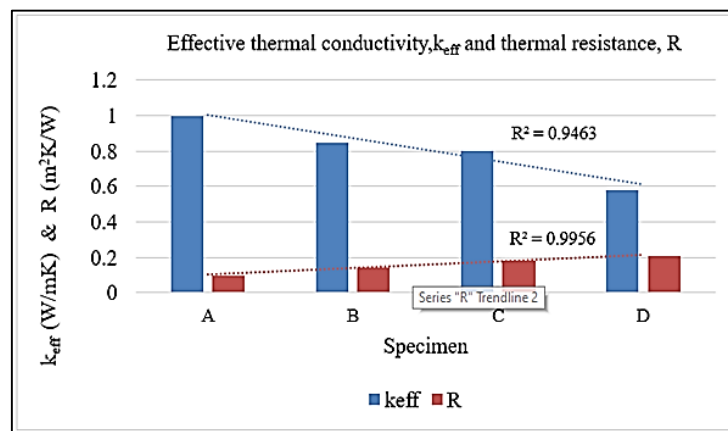


**Fig. 10.** Relationship of  $k_{eff}$  and R for each wall specimens

#### 4. Conclusions

The conclusions drawn from this paper are as follows:

- i. Cement plaster and insulation materials were found to significantly contribute to the thermal performance of a masonry wall, leading to enhanced thermal comfort in buildings.
- ii. A 20mm two-sided cement plaster exhibited better heat transmission restraint at specific spots, as evidenced by achieving the highest spot temperature difference in the thermal test. On the other hand, a 20mm polystyrene board demonstrated superior performance in insulating a wall surface in all directions, resulting in the largest average surface temperature difference among all the specimens.

- iii. Polystyrene board exhibited greater insulation capabilities compared to cement plaster of the same thickness. A 20mm polystyrene board reduced heat transfer by up to 51.7%, while a 20mm one-sided cement plaster achieved a reduction of only up to 29%.
- iv. The thickness of the cement plaster applied directly influenced the thermal resistance of the wall. A 20mm two-sided cement plastered wall demonstrated a higher thermal resistance value and effectively limited heat transmission when compared to a 20mm one-sided cement plastered wall.

### Acknowledgement

This research was funded by a grant from Ministry of Higher Education under Fundamental Research Grant Scheme, UTM, FRGS/1/2023/TK01/UTM/02/3 or R.J130000.7822.5F671 and UTM Fundamental Research Grant of Q.J130000.3822.22H54.

### References

- [1] Ozturk, Savas. "Optimization of thermal conductivity and lightweight properties of clay bricks." *Engineering Science and Technology, an International Journal* 48 (2023): 101566. <https://doi.org/10.1016/j.jestch.2023.101566>
- [2] Zilberberg, E., P. Trapper, I. A. Meir, and S. Isaac. "The impact of thermal mass and insulation of building structure on energy efficiency." *Energy and Buildings* 241 (2021): 110954. <https://doi.org/10.1016/j.enbuild.2021.110954>
- [3] Rodrigues, Eugénio, Nazanin Azimi Fereidani, Marco S. Fernandes, and Adélio R. Gaspar. "Diminishing benefits of thermal mass in Iranian climate: Present and future scenarios." *Building and Environment* 258 (2024): 111635. <https://doi.org/10.1016/j.buildenv.2024.111635>
- [4] Kaddouri, Hicham, Abderrahim Abidouche, Mohamed Saidi Hassani Alaoui, Ismael Driouch, Said Hamdaoui, and Abdelouahad Ait Msaad. "Study of the energy, economic, environmental, and thermal comfort impact of the integration of hemp concrete and hemp plaster in a residential building envelope in Morocco." *Journal of Advanced Research in Numerical Heat Transfer* 23, no. 1 (2024): 1-27. <https://doi.org/10.37934/arnht.23.1.127>
- [5] Li, Yongcai, Xiaohan Tao, Yaqin Zhang, and Wuyan Li. "Combining use of natural ventilation, external shading, cool roof and thermal mass to improve indoor thermal environment: Field measurements and simulation study." *Journal of Building Engineering* 86 (2024): 108904. <https://doi.org/10.1016/j.jobe.2024.108904>
- [6] Hou, Liqiang, Yan Liu, Yiyu Zhu, Lingzhi Liu, Xiaolong Zhao, and Liu Yang. "Thermal performance of cavity masonry wall structures in the solar rich areas of Western China." *Journal of Building Engineering* 86 (2024): 108797. <https://doi.org/10.1016/j.jobe.2024.108797>
- [7] Zakaria, Nurul Mardhiyah, Mohamad Alif Omar, and Azfarizal Mukhtar. "Numerical study on the thermal insulation of smart windows embedded with low thermal conductivity materials to improve the energy efficiency of buildings." *CFD Letters* 15, no. 2 (2023): 41-52. <https://doi.org/10.37934/cfdl.15.2.4152>
- [8] Kurmus, Halenur, and Abbas Mohajerani. "Energy savings, thermal conductivity, micro and macro structural analysis of fired clay bricks incorporating cigarette butts." *Construction and Building Materials* 283 (2021): 122755. <https://doi.org/10.1016/j.conbuildmat.2021.122755>
- [9] Srimuang, Kantaphong, Thanongsak Imjai, Fetih Kefyalew, Sudharshan N. Raman, Reyes Garcia, and Sandeep Chaudhary. "Thermal and acoustic performance of masonry walls with phase change materials: A comparison of scaled-down houses in tropical climates." *Journal of Building Engineering* 82 (2024): 108315. <https://doi.org/10.1016/j.jobe.2023.108315>
- [10] Challamel, Noël, Cécile Grazide, Vincent Picandet, Arnaud Perrot, and Yingyan Zhang. "A nonlocal Fourier's law and its application to the heat conduction of one-dimensional and two-dimensional thermal lattices." *Comptes Rendus. Mécanique* 344, no. 6 (2016): 388-401. <https://doi.org/10.1016/j.crme.2016.01.001>
- [11] Lebon, Georgy, D. Jou, and P. C. Dauby. "Beyond the Fourier heat conduction law and the thermal no-slip boundary condition." *Physics Letters A* 376, no. 45 (2012): 2842-2846. <https://doi.org/10.1016/j.physleta.2012.09.034>
- [12] Pásztor, Zoltán. "An overview of factors influencing thermal conductivity of building insulation materials." *Journal of Building Engineering* 44 (2021): 102604. <https://doi.org/10.1016/j.jobe.2021.102604>
- [13] Ermolaev, Vladimir. "Heat Transfer Mechanisms. Thermal Conductivity." In *Thermal Engineering*, pp. 117-129. Cham: Springer Nature Switzerland, 2024. [https://doi.org/10.1007/978-3-031-50373-3\\_12](https://doi.org/10.1007/978-3-031-50373-3_12)
- [14] Hamidi, Youssef, Mustapha Malha, and Abdellah Bah. "Analysis of the thermal behavior of hollow bricks walls filled with PCM: Effect of PCM location." *Energy Reports* 7 (2021): 105-115. <https://doi.org/10.1016/j.egy.2021.08.108>

- [15] Hattan, Hamed Abbasi, Mortaza Madhkhan, and Afshin Marani. "Thermal and mechanical properties of building external walls plastered with cement mortar incorporating shape-stabilized phase change materials (SSPCMs)." *Construction and Building Materials* 270 (2021): 121385. <https://doi.org/10.1016/j.conbuildmat.2020.121385>
- [16] Zhou, Kun, Jinfeng Mao, Yong Li, Hua Zhang, and Zhongkai Deng. "Prediction and parametric analysis of 3D borehole and total internal thermal resistance of single U-tube borehole heat exchanger for ground source heat pumps." *Energy and Built Environment* 4, no. 2 (2023): 179-194. <https://doi.org/10.1016/j.enbenv.2021.11.001>
- [17] Yang, Jianming, Huijun Wu, Xinhua Xu, Gongsheng Huang, Jian Cen, and Yuying Liang. "Regional climate effects on the optimal thermal resistance and capacitance of residential building walls." *Energy and Buildings* 244 (2021): 111030. <https://doi.org/10.1016/j.enbuild.2021.111030>
- [18] Irsyad, Muhammad, Ari Darmawan Pasek, Yuli Setyo Indartono, and Adi Widya Pratomo. "Heat transfer characteristics of building walls using phase change material." In *IOP Conference Series: Earth and Environmental Science*, 60, no. 1, p. 012028. IOP Publishing, 2017. <https://doi.org/10.1088/1755-1315/60/1/012028>
- [19] Oliveira, A. V. S., A. Avrit, and Michel Gradeck. "Thermocouple response time estimation and temperature signal correction for an accurate heat flux calculation in inverse heat conduction problems." *International journal of heat and mass transfer* 185 (2022): 122398. <https://doi.org/10.1016/j.ijheatmasstransfer.2021.122398>
- [20] Gupta, Manglesh Kumar, Pushpendra Kumar Singh Rathore, Rajan Kumar, and Naveen Kumar Gupta. "Experimental analysis of clay bricks incorporated with phase change material for enhanced thermal energy storage in buildings." *Journal of Energy Storage* 64 (2023): 107248. <https://doi.org/10.1016/j.est.2023.107248>